Geochimica et Cosmochimica Acta Vol. 55, pp. 1549–1562

0016-7037/91/$3.00 + .00

Sorption of divalent metals on calcite

J. M. ZACHARA, C. E. COWAN, and C. T. RESCH
Geosciences Department, Pacific Northwest Laboratory, Richland, WA 99352, USA

(*Received June* 6, 1990; *accepted in revised form April* 4, 1991)

Abstract—The sorption of seven divalent metals (Ba, Sr, Cd, Mn, Zn, Co, and Ni) was measured on calcite over a large initial metal (Me) concentration range (10^{-8} to 10^{-4} mol/L) in constant ionic strength ($I = 0.1$), equilibrium $CaCO_3$(s)-$CaCO_3$(aq) suspensions that varied in pH. At higher initial Me concentrations (10^{-5} to 10^{-4} mol/L) geochemical calculations indicated that the equilibrium solutions were saturated with discrete solid phases of the sorbates: $CdCO_3$(s), $MnCO_3$(s), $Zn_5(OH)_6(CO_3)_2$(s), $Co(OH)_2$(s), and $Ni(OH)_2$(s), implying that aqueous concentrations were governed by solubility. However, significant sorption of all the metals except for Ba and Sr was observed at aqueous concentrations below saturation with Me-solid phases. Divalent metal ion sorption was dependent on aqueous Ca concentration, and the following selectivity sequence was observed: Cd > Zn ≥ Mn > Co > Ni ≫ Ba = Sr. The metals varied in their sorption reversibility, which was correlated with the single-ion hydration energies of the metal sorbates. The strongly hydrated metals (Zn, Co, and Ni) were most desorbable. A sorption model that included aqueous speciation and Me^{2+}-Ca^{2+} exchange on cation-specific surface sites was developed that described most of the data well. The chemical nature of the surface complex used in this model was unspecified and could represent either a hydrated or dehydrated surface complex, or a surface precipitate. A single exchange constant for Cd, Mn, Co, and Ni could describe the sorption of that metal over a wide range in pH, Ca concentration, and surface concentration. Zinc, however, exhibited nonlinear sorption behavior and required exchange constants that varied with surface coverage. Our data suggested that (i) Cd and Mn dehydrate soon after their adsorption to calcite and form a phase that behaves like a surface precipitate, and (ii) Zn, Co, and Ni form surface complexes that remain hydrated until the ions are incorporated into the structure by recrystallization.

INTRODUCTION

DIVALENT METALLIC CATIONS (Me^{2+}) sorb to the surface of calcite (MORSE, 1986), thereby influencing their aqueous-phase concentrations in calcareous environments. Sorption, defined generally as a surface localization process irrespective of mechanism (SPOSITO, 1986), represents a potentially significant metal-scavenging process in aquatic, marine, and ground-water environments and in mineral waste systems (FULLER and DAVIS, 1987; DUDLEY et al., 1988; ZACHARA et al., 1989). Sorbed metallic cations may be incorporated into the calcite lattice, reflect the geochemical conditions of formation (REEDER and PROSKY, 1986; PINGITORE and EASTMAN, 1986; REEDER and GRANS, 1987), and provide a future source of these same metals upon dissolution of calcite.

Divalent metallic cations at low aqueous concentration first associate with the calcite surface via an adsorption reaction whose identity and stoichiometry has not been fully resolved (FRANKLIN and MORSE, 1983; KORNICKER et al., 1985; DAVIS et al., 1987; ZACHARA et al., 1988). The term adsorption is used here according to the definition of SPOSITO (1986), as representing the interfacial accumulation of sorbate as a surface complex, without development of a three-dimensional molecular arrangement. It has been speculated that the adsorption reaction occurs via exchange with Ca in exposed structural (lattice) sites (KOSS and MOLLER, 1974) or by complexation to carbonate groups bound in a disordered, hydrated surface layer (LAHANN and SIEBERT, 1982; DAVIS et al., 1987; ZACHARA et al., 1988).

On calcite, the fate of the adsorbed metal ions with time appears to vary between different sorbates and is complex. For example, Zn formed surface complexes that were desorbable from calcite after 48 h (ZACHARA et al., 1988), while adsorbed Cd and Mn have been reported to rapidly transform to a surface phase exhibiting slow desorption rates (MCBRIDE, 1980; DAVIS et al., 1987; PAPADOPOULOS and ROWELL, 1988). The Mn and Cd surface phases have been described by the noted authors variously as chemisorbed complexes, surface precipitates, and $MeCO_3$(s)-$CaCO_3$(s) solid solutions, attesting to ambiguity in terminology applied to the adsorption-precipitation boundary (see COREY, 1981; SPOSITO, 1986) as well as incomplete molecular understanding of their chemical nature. Under equilibrium conditions with respect to calcite solubility, surface associated metal ions may be incorporated into the calcite structure, as a coprecipitate, by recrystallization (LORENS, 1981; DAVIS et al., 1987; ZACHARA et al., 1988). Discrete $MeCO_3$ or basic-metal carbonate precipitates may form on the calcite surface in more concentrated metal solutions (MCBRIDE, 1979, 1980; GLASNER and WEISS, 1980; KAUSHANSKY and YARIV, 1986; PAPADOPOULOS and ROWELL, 1988; ZACHARA et al., 1989).

The factors controlling metal ion sorption and adsorption selectivity on calcite are not fully understood because individual investigators have studied single metal sorbates (see all references above). Comparisons between these studies are difficult because of the use of different calcite sorbents, electrolyte solutions, and experimental procedures, all of which can exert a strong influence on the reactions responsible (adsorption, precipitation) for metal cation sorption to calcite. Thus, trends have not been established between sorption behavior, sorbate properties, and the solution composition that could be used to determine the sorption mechanism and the chemical basis for surface selectivity.

The present study examines the sorption of seven different

divalent metal ions on calcite over short contact times to minimize the complicating influence of recrystallization. Metal ions varying in ionic radius, hydration energy, and other properties were used to (i) determine the chemical factors influencing selectivity for the calcite surface and (ii) provide further insights on relative contributions of adsorption and precipitation to sorption over concentration ranges relevant to contaminant geochemistry. A equilibrium chemical model based on Me^{2+}-Ca^{2+} surface exchange on calcite was developed and applied to describe the effects of Ca activity and pH on metal cation sorption. The results were used to evaluate the conceptual veracity of several recently proposed models of coupled adsorption/precipitation reactions on calcite (DAVIS et al., 1987; COMANS and MIDDELBURG, 1987; WERSIN et al., 1989).

EXPERIMENTAL METHODS

The Calcite Sorbent

Reagent-grade calcite ($CaCO_3$(s), Fisher Scientific) was aged by storing 0.5 kg of $CaCO_3$(s) in 14 L of 0.02 mol/L $NaHCO_3$(aq) for 30 days according to the procedure of REDDY and NANCOLLAS (1971). The suspension was agitated daily during this period. The aging process establishes calcite crystallites with a more uniform particle diameter then reagent-grade calcite, through recrystallization. Recrystallization refers to a process, that occurs in saturated solution and is driven by surface free energy, where smaller crystallites and surfaces with defects dissolve and reprecipitate as energetically more stable forms. Following the aging period, the $CaCO_3$(s) was separated from the storage solution by filtration and then lyophilized. All isotopic exchange and metal ion sorption experiments were performed with this aged calcite. The aged $CaCO_3$(s) was 100% calcite by X-ray diffraction and had a BET surface area as measured by triple-point krypton adsorption of approximately 0.20 m^2/g. This surface area was at the lower limit of our measurement capability. Electron microscopy showed that the crystallites were rhombohedral in morphology and were intergrown. The average length of the calcite rhoms estimated from electron microscopy was approximately 9.0 μm.

Equilibrium Calcite Solutions

Eight solutions in equilibrium with calcite ($CaCO_3$(s)-$CaCO_3$(aq)) ranging from pH 7.0 to pH 9.5 at 25°C were prepared by first mixing $HClO_4$, $Ca(ClO_4)_2$, $NaClO_4$, $NaHCO_3$, and NaOH to achieve the desired solution composition and pH and a total ionic strength of 0.1. These solutions were then allowed to equilibrate with $CaCO_3$(s) in contact with atmospheric CO_2(g) (pCO_2 = 3.5) for 2 weeks. The equilibrium solutions were stored in contact with new $CaCO_3$(s) until being used in the sorption experiments. Further details on the synthesis of similar solutions can be found in ZACHARA et al. (1988). The composition of the equilibrium calcite solutions are provided in Appendix Table I. Calculations using the geochemical code MINTEQ (FELMY et al., 1984) with the equilibrium constants tabulated in Appendix Tables II and III confirmed that the solutions were in equilibrium with calcite.

Cation-Specific Surface Sites

The isotopic exchange of ^{45}Ca was measured on calcite in equilibrium $CaCO_3$(s)-$CaCO_3$(aq) solutions at pH 8.3, 8.7, 9.0, and 9.3 to determine, by isotopic dilution, the concentration of Ca on the calcite surface.

Calcite (1.000 g) was placed into tared 25-mL polycarbonate centrifuge tubes, and 10 mL of the appropriate equilibrium $CaCO_3$(s)-$CaCO_3$(aq) solution (0.22 μm filtered) was added to each tube to yield a 100 g/L suspension. These tubes were agitated overnight at 25°C. The tubes were then reweighed, the $CaCO_3$(s) was allowed to settle, and 1 mL of the supernate was removed and placed into a tared 5-mL polystyrene tube. The 5-mL tubes were weighed, 300,000 cpm of carrier-free ^{45}Ca was added, and the tubes were remixed and weighed again. Two 100-μL aliquots were removed for counting into tared scintillation vials, and the 5-mL tubes were reweighed to determine pre-spike mass. The ^{45}Ca spike was then rapidly added to the calcite suspension, and the final mass of the 5-mL tube was recorded after spiking to determine residual counts. Each 25-mL tube then contained approximately 25,000 cpm/g of suspension. This procedure enabled accurate determination of the specific activity of ^{45}Ca in each of the tubes at the start of the isotopic-exchange experiment.

The tubes were rolled end-over-end to ensure good mixing, and duplicate 25-mL tubes were sacrificed at each pH after 4, 8, 12, 24, and 48 h. The tubes were centrifuged at 4800 rcf for 10 min, then aliquots were removed, by mass, for scintillation counting. Final pH was measured using a Ross combination pH electrode.

Sorption Edges

Sorption of 10^{-7} mol/L Ba, Sr, Cd, Mn, Zn, Co, and Ni was measured on calcite (@25 g/L, ~5.00 m^2/L) in each of the eight different equilibrium $CaCO_3$(s)-$CaCO_3$(aq) solutions. The experiments were performed by placing 20 mL (weighed to 0.001 g) of the appropriate 0.22-μm filtered $CaCO_3$(s)-$CaCO_3$(aq) solution into a 35-mL polycarbonate centrifuge tube into which calcite was added (0.50 g recorded to 0.001 g). The $CaCO_3$(s) suspensions were agitated overnight and the following morning were spiked with radiolabeled, 10^{-5} mol/L $MeCl_2$ solutions (at pH 4) to yield a final concentration of 10^{-7} mol/L with 15,000 cpm/g of solution. The concentration of the radiolabeled 10^{-5} mol/L $MeCl_2$ spiking solution was determined by ICAP. The $MeCl_2$ spike mass was recorded to 0.001 g to quantify the initial Me^{2+} concentration. Replicate samples and replicate reagent blanks were used at each different pH for each different metal. The tubes were then agitated for 24 h at 25°C and were centrifuged at 4800 rcf for 10 min for phase separation. Aliquots of the supernatant were removed for scintillation counting to quantify the final Me^{2+} concentration. Final pH of each sample and blank was measured with stirring, using a Ross combination electrode; a 20-min stabilization period was required. Four samples at different pH values were removed from each metal series to quantify final levels of Ca and other cations in the equilibrium solution.

Desorption

To evaluate the lability of the surface complex, desorption was measured at an initial concentration of 10^{-7} mol/L Me^{2+}. The procedure was designed to minimize "apparent desorption" that could arise from dissolution of the calcite surface.

The Me^{2+} ions at 10^{-7} mol/L were sorbed on calcite (25 g/L) in 20-mL suspensions of $CaCO_3$(s)-$CaCO_3$(aq) at pH 8.7. Metal sorption was at or near its maximum value at this pH. Sixteen individual polycarbonate tubes were used for each metal. The $CaCO_3$(s) equilibration and the Me^{2+} spiking procedures were identical to those already described.

After a 24-h equilibration, the amount of sorption and the pH were determined. The equilibrium sorbate solutions were removed after centrifugation and their masses recorded. An identical mass (~20 g) of $CaCO_3$(s)-$CaCO_3$(aq) solution at lower pH (Co, Ni and, Mn–pH 7.6; Zn and Cd–pH 7.2) was then added to the Me^{2+}-loaded calcite to induce desorption. Before addition, the new $CaCO_3$(s)-$CaCO_3$(aq) solution was spiked with Me^{2+} to yield an aqueous Me^{2+} concentration identical to that present in the original equilibrium solution at pH 8.7. Thus, the total concentration of Me^{2+} in the desorption experiment (aqueous plus sorbed) was identical to that in the sorption experiment. Replicate tubes were then sacrificed at 2, 4, 6, 8, 12, 24, and 48 h after electrolyte replacement.

Sorption Isotherms

Sorption isotherms for Cd, Mn, Zn, Co, and Ni were measured over the initial concentration range of 10^{-4} to 10^{-8} mol/L. The isotherms were performed in one of two different $CaCO_3$(s)-$CaCO_3$(aq) solutions; lower-pH solutions were used for the more strongly sorbing Me^{2+} ions (Cd–pH 7.4; Zn–pH 7.4 and pH 8.4; and Mn, Co, and

Ni–pH 8.4). It was fully expected and desired that precipitation of discrete solid phases [$CdCO_3$, $MnCO_3$, $Zn_5(OH)_6(CO_3)_2$, $Co(OH)_2$, $Ni(OH)_2$] would occur at higher initial sorbate concentrations (e.g., $>10^{-5}$ mol/L initial concentration).

The sorption isotherms were measured in 20 mL suspensions with calcite at 25 g/L. The procedures for pre-equilibration, mass quantification, sorbate spiking, and equilibration were identical to those for the pH edges. A separate spiking solution was used for each initial concentration and these were diluted by a factor of 100 in spiking (i.e., 10^{-6} to yield 10^{-8}, etc.). Initial radiolabel activity was 15,000 cpm/g of solution. Replicate samples and reagent blanks were used for each metal at each initial concentration. Final pH was measured on all samples. The equilibrium solution composition was analyzed by ICAP. The final Me^{2+} concentrations were quantified by scintillation counting and were corroborated by ICAP analyses when their concentrations were above the ICAP detection limit. The equilibrium code MINTEQ (FELMY et al., 1984) was used to determine the saturation states of the final experimental solution compositions with respect to the solubilities of Me^{2+} solids according to the equilibrium constants in Tables II and III of the Appendix.

RESULTS AND DISCUSSION

Concentration of Cation-Specific Surface Sites

The fraction of ^{45}Ca exchanged on the surface of calcite at 100 g/L (f_{ex}, Fig. 1a) varied with pH and aqueous Ca concentration according to the mass law equation

$$Ca(s) + {}^{45}Ca^{2+}(aq) = {}^{45}Ca(s) + Ca^{2+}(aq) \quad (1)$$

where (s) denotes surface associated Ca and the equilibrium constant (K) for the reaction is about 1. Consistent with reaction (1), the total fraction exchanged (Fig. 1a) was greatest at higher pH, where the aqueous concentration of Ca^{2+} was lowest. The change in f_{ex} with Ca concentration in Fig. 1a was in agreement with the following relationship derived from Eqn. (1):

$$f_{ex} = [Ca(s)]/([Ca(s)] + [Ca^{2+}(aq)]) \quad (2)$$

where all terms in Eqn. (2) are in mol/L.

The isotopic exchange of ^{45}Ca was nearly complete within 2 h; however, a subsequent slower time-dependent increase in f_{ex} was observed (Fig. 1a). The rapid initial uptake of ^{45}Ca has been ascribed to both exchange with Ca on a monolayer of exposed lattice sites (MOLLER and SASTRI, 1974) or within a partially hydrated calcite surface layer (DAVIS et al., 1987). The slower time-dependent increase in f_{ex} has been postulated to result from lattice penetration (INKS and HAHN, 1967) and/or surface recrystallization of ^{45}Ca ions bound in the surface layer (LORENS, 1981; MOZETO et al., 1984; DAVIS et al., 1987).

The concentrations of Ca surface sites [$Ca_{(s)}$ in mol/g] was estimated at each pH after 24 h of exchange according to the equation:

$$Ca_{(s)} = \{([^{45}Ca]s \times [Ca^{2+}]aq)/[^{45}Ca]aq\}/CaCO_3(s) \quad (3)$$

where [^{45}Ca]s and [^{45}Ca]aq are in cpm/L, [Ca^{2+}]aq is the total analytical concentration of Ca in mol/L, and $CaCO_3$(s) is in g/L. The calculated value of $Ca_{(s)}$ represents the sum of labile Ca in the surface layer of the solid phase and that localized in the diffuse layer surrounding the particles. Our $Ca_{(s)}$ values over the pH range of 8.4–9.0 (Fig. 1b) compared favorably with $Ca_{(s)}$ values of 2.3×10^{-6} mol/g and 3.3×10^{-6} mol/g determined by DAVIS et al. (1987) for calcite in 0.1 mol/L NaCl at pH 8.00 and artificial groundwater at pH 8.3, respectively. Since aqueous speciation effects cancel in Eqn. (3), the increase in $Ca_{(s)}$ at and above pH 9.0 (Fig. 1b) may be due to Ca^{2+} (i) adsorption to CO_3 surface sites or (ii) localization in the diffuse double layer as the surface of calcite is reported to carry net negative charge above pCa = 4.4 (FOXALL et al., 1979).

For the purposes of subsequent sorption modelling the $Ca_{(s)}$ values over the pH range of 8.4–9.0 were averaged to yield a value of 3.6×10^{-6} mol/g. This value was assumed to represent the concentration of Ca in the uppermost surface layer or layers on the calcite surface (termed X_t). This surface density of Ca yields an estimate of surface area (0.4 m^2/g) that exceeds the measured value (0.20 m^2/g), if these $Ca_{(s)}$ sites are assumed to represent structural Ca ions on the cleavage face as proposed by MOLLER and SASTRI (1974). DAVIS et al. (1987) noted that isotopic exchange measurements on calcite provided inconsistent estimates of calcite surface area and proposed that the isotopic exchange occurs within a hydrated, multiatomic layer on the calcite surface. The isotopic exchange of ^{45}Ca and ^{32}P on hydroxyapatite also defines an approximate crystalline monolayer near the ZPC (KUKURA et al., 1972), but surface concentrations of Ca^{2+} and PO_4^{3-} vary significantly with both pH and displacement from the ZPC. Recent LEED photographs (HOCHELLA, 1990; STIPP and HOCHELLA, 1991) suggest that the surface hydrated layer on calcite, if present, is unlikely to exceed two monolayers in depth.

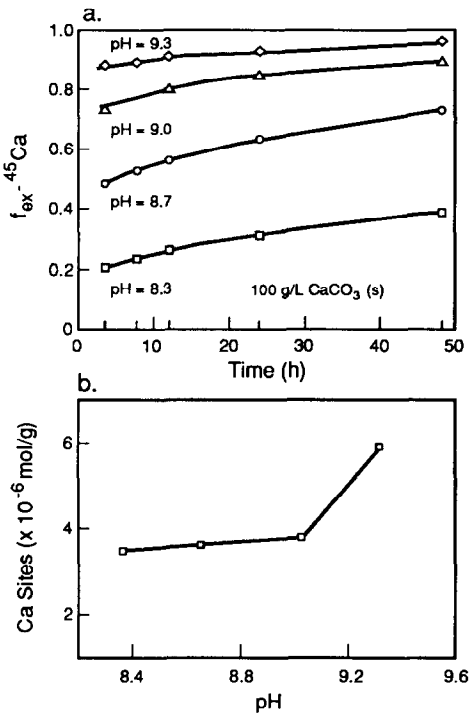

FIG. 1. (a) Isotopic exchange of $^{45}Ca^{2+}$ on calcite in equilibrium $CaCO_3$(s)-$CaCO_3$(aq) suspensions at a solids concentration of 100 g/L $CaCO_3$(s), and (b) the concentration of cation-specific surface sites ($Ca_{(s)}$) on aged calcite estimated from the exchange data in (a) using Eq. (3).

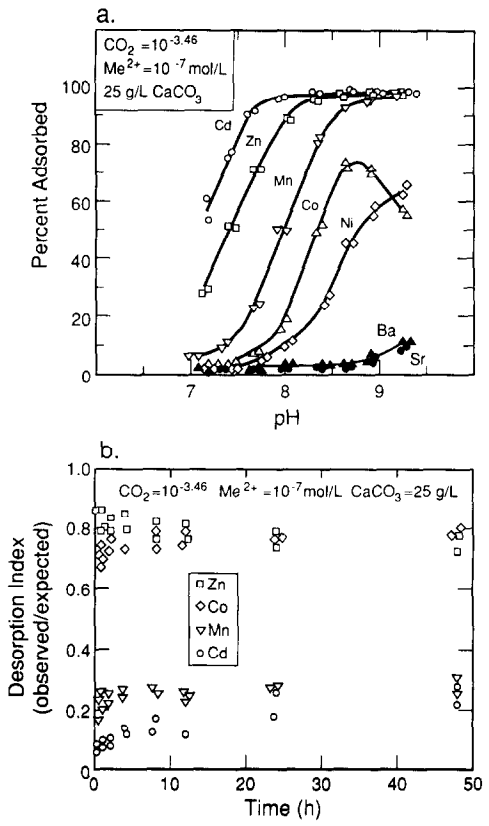

FIG. 2. (a) Fractional sorption of divalent metals on calcite in equilibrium $CaCO_3$(s)-$CaCO_3$(aq) suspensions over a range in pH and Ca concentrations. Solids concentration was 25 g/L; ionic strength was approximately 0.1. (b) Desorption of sorbed metals in equilibrium $CaCO_3$(s)-$CaCO_3$(aq) suspensions after change in aqueous Ca concentration. Equilibration time for sorption was 24 h. Desorption index is as defined in text.

Sorption Behavior

The fractional sorption of all the metals increased with increasing pH (Fig. 2a). The increase in sorption paralleled a decrease in the aqueous concentration of Ca maintained by calcite solubility. We have observed identical patterns of sorption behavior on several different calcite sorbents, indicating that these results are not a relict of unknown impurities that could potentially exist in the calcite used in this study. It has been previously shown that the sorption on calcite of both Co (KORNICKER et al., 1985) and Zn (ZACHARA et al., 1988) appears to occur in competition with Ca. Furthermore, various studies have suggested that the surface of calcite is in exchange equilibrium with major and minor solutes in the aqueous phase (MOLLER, 1973; MOLLER and SASTRI, 1974; MUCCI and MORSE, 1983). Although the sorption behavior shown in Fig. 2a could arise from the precipitation of Me-carbonate, Me-hydroxide, or basic-carbonate solid phases, the final concentrations for all the metals were significantly below those required to precipitate these solids. The fractional sorption data for all the metals in Fig. 2a therefore appeared consistent with the surface-exchange reaction proposed by ZACHARA et al. (1988) for Zn:

$$Ca(surface) + Me^{2+}(aq) = Me(surface) + Ca^{2+}(aq). \quad (4)$$

Metals with ionic radii (r_x) greater than Ca (i.e., Ba and Sr; Table 1) that form anhydrous $MeCO_3$(s) solids with aragonite structure were weakly sorbed by calcite (Fig. 2a). In contrast, metals with r_x smaller than Ca (Cd, Mn, Zn, Co, and Ni; Table 1) that form $MeCO_3$(s) with calcite structure were more strongly sorbed and showed metal-specific selectivity for the surface (Fig. 2a). The selectivity of calcite for the Me^{2+} ions generally decreased as $\Delta r_x (r_{x\text{-Me}} - r_{x\text{-Ca}})$ increased. That is, Cd was most strongly sorbed ($\Delta r_x = -0.02$), while Ni

Table 1. Selected properties of the metal ion sorbates and their calculated surface exchange constants.

Metal	r_x (Å)	Δ-r_x[a] (Å)	ΔG_H[b] (kcal/mol)	$MeCO_3$(s)[c] (log K)	$MeCO_3^o$(aq)[c] (log K)	$MeHCO_3^+$(aq)[c] (log K)	X-Me[d] (log $^cK_{ex}$)
Ba	1.34	0.35	-315.1	8.58			-1.93
Sr	1.12	0.13	-345.9	9.25			-2.04
Ca	0.99	0	-380.8				0
Cd	0.97	-0.02	-430.5	12.1	4.0	2.07	3.02
Mn	0.80	-0.19	-437.8	10.4	4.1	1.27	1.31
Zn	0.74	-0.25	-484.6	10.8	4.8	2.1	2.43
Co	0.72	-0.27	-479.5	10.1	3.17	1.39	0.56[e]
Ni	0.69	-0.30	-494.2	6.84	4.83	2.14	0.51[f]

a Δ ionic radius = Me^{2+} ionic radius - Ca^{2+} ionic radius

b ΔG_H = single-ion Gibbs free energies of hydration from BURGESS (1978)

c sources of data given in Appendix Table II

d $X\text{-}Ca + Me^{2+} = X\text{-}Me + Ca^{2+}$ $^cK_{ex}$
where X is a cation specific surface site and
$$^cK_{ex} = \frac{(Ca^{2+})[X\text{-}Me]}{(Me^{2+})[X\text{-}Ca]}$$
values for X-Me and X-Ca are in mol/L

e value fit without data at pH 8.9 and 9.3; $^cK_{ex}$ is 0.39 if all points included or 0.57 if all points are included along with $Co(CO_3)_2^{2-}$(aq).

f best fit to the data in Fig. 6a is obtained with the noted constant and with $^cK_{ex}$ - NiOH = 1.06

was least strongly sorbed ($\Delta r_x = -0.30$). Manganese ($\Delta r_x = -0.19$) and Zn ($\Delta r_x = -0.25$), however, showed reversed selectivity with respect to this size trend (Fig. 2a).

Desorption

The three metals Zn, Co, and Ni were desorbable from calcite (Fig. 2b). A desorption index (DI), where DI = [equilibrium mol Me^{2+}/g at pH 7.6 (Co, Mn, and Ni) or pH 7.2 (Zn and Cd) with initial $Me^{2+} = 10^{-7}$ mol/L]/[mol Me^{2+}/g in the desorption experiment at time t], approaching 1.0 signifies a labile surface complex, while a DI of 0.1 indicates irreversibility. Generally, the desorption of Zn, Co (Fig. 2b), and Ni (not shown) was complete within 8 h and showed no appreciable increase with time up to 48 h. ZACHARA et al. (1988) also observed sorption reversibility for Zn on calcite in comparable experiments. The ~20% of these sorbed metals that was not desorbable (Fig. 2b), probably represented sorbate that was incorporated into the $CaCO_3$(s) by lattice penetration or recrystallization. This non-desorbable fraction was similar to or slightly less than the fraction of $^{45}Ca^{2+}$ fixed over a comparable time period (Fig. 1a).

Manganese and cadmium, in contrast, showed limited sorption reversibility after 48 h (Fig. 2b). Only 10 to 25% of the sorbed concentration of these two metals was desorbable. Cadmium, the most strongly sorbed metal, and the metal with r_x closest to Ca^{2+}, was least desorbable. However, ease of desorption was not simply a function of sorption strength; although Zn was sorbed more strongly than Mn (Fig. 2a), Zn sorption was reversible. The final metal concentrations were calculated with MINTEQ to be below those required for saturation with $CdCO_3$(s) and $MnCO_3$(s), indicating that discrete $MeCO_3$(s) precipitation was not cause for sorption irreversibility. DAVIS et al. (1987) also observed limited desorption of Cd from calcite after 24 h of sorption and their desorption index was similar to that shown in Fig. 2b. DAVIS et al. (1987) observed more rapid desorption rates if sorption contact periods were shortened. These authors postulated that Cd diffused within a surface layer and was incorporated into the crystalline structure as a solid solution (as defined by COREY, 1981) as new crystalline material formed from the hydrated layer. MCBRIDE (1979) suggested that Mn is chemisorbed by calcite at aqueous Mn^{2+} concentrations below saturation with $MeCO_3$(s). Chemisorption involves the formation of strong chemical bonds similar to those occurring in precipitates (COREY, 1981). MCBRIDE (1979) likened this chemisorption to the formation of a two-dimensional Me-Ca solid solution.

The average desorption index after 8 h for Cd, Zn, Mn, Co, and Ni correlated well with the single-ion hydration energies (ΔG_H, Table 1) of the metal sorbates, Fig. 3. The high hydration energies of Co, Ni, and Zn apparently prevent dehydration of these ions on the calcite surface or within the surface layer, and they allow the continued persistence of these ions as partly hydrated, exchangeable surface complexes. This observation was consistent with the slow observed precipitation rates (at room temperature and pressure) of anhydrous metal carbonates of the strongly hydrated divalent metal cations (e.g., Mg, LIPPMANN, 1973, pp. 76–87; Zn, SCHINDLER et al., 1968). The desorption data suggest that

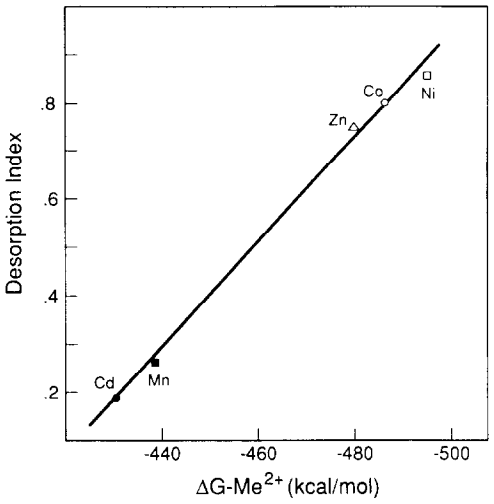

FIG. 3. Relationship between the average desorption index after 8 h of desorption and the single-ion hydration energies of the divalent metal cations.

sorbed hydrated metal ions distributed on the calcite surface or within a surface layer undergo exchange equilibria with the aqueous phase within 4–8 h. In contrast, the lower hydration energies of Cd and Mn allow these metals to form a dehydrated or partially dehydrated surface phase or complex containing $MeCO_3$ bonds. Cadmium and manganese apparently form these dehydrated surface phases rapidly, because there was limited desorption at the first time of observation (e.g., 2 h, Fig. 2b). FRANKLIN and MORSE (1983) concluded that Mn dehydration and formation of a chemical bond on the surface controlled Mn sorption kinetics on calcite over intermediate time periods.

Sorption and Exchange Isotherms

Sorption isotherms were measured for Cd, Mn, Zn, Co, and Ni at two different pH values (7.4 and 8.4, Fig. 4a) to (i) maximize the aqueous Me^{2+} concentration range over which discrete Me-solid phase precipitation would not occur and (ii) maintain fractional adsorption between 50 and 95% for better measurement statistics. The final concentration range in the isotherms that corresponds with the sorption-edge experiments in Fig. 2a ranged from $10^{-7.85}$ to $10^{-7.1}$ mol/L and is noted on the ordinate in Fig. 4a. Sorption isotherms for all the metals in Fig. 4a were controlled by precipitation of discrete Me-containing solid phases above a final equilibrium concentration of approximately 10^{-6} mol/L (discussed subsequently in Fig. 4b). Isotherms for Cd, Mn, Co, and Ni were linear on a log-log basis below an equilibrium concentration of 10^{-6} mol/L and exhibited a slope of near unity. In contrast, Zn isotherms exhibited non-unit slope at both pH values.

The aqueous concentration data from the isotherm experiments (Fig. 4a) were speciated using MINTEQ and the equilibrium constants in Appendix Table II. The calculated single-ion activities for the uncomplexed divalent metal species (Me^{2+}) were used along with the concentration of cation-specific surface sites ($X_t = 3.46 \times 10^{-6}$ mol/g, Fig. 1b) to construct ion exchange isotherms (Fig. 4b) of the form:

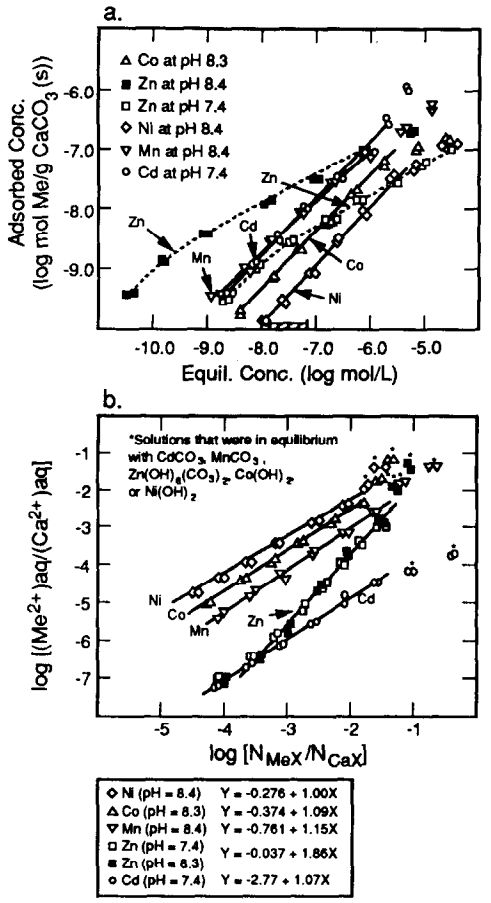

FIG. 4. Sorption isotherms of divalent metals on calcite. (a) Unspeciated isotherms based on concentration-change measurements. The pH variation between metals is noted. Zinc isotherms are connected by dotted lines. (b) Speciated exchange isotherms based on Eqn. (5) and data in (a), complexation constants in Appendix Table II, and surface site concentration (X_t) determined in Fig. 1b.

$$\log [(Me^{2+})aq/(Ca^{2+})aq] = \log K_{ex} + n \log [N_{MeX}/N_{CaX}]. \quad (5)$$

In Eqn. (5), N_{MeX} is the mole number (fraction) of metal sorbate on the cation specific surface site,

$$N_{MeX} = [\text{sorbed } Me^{2+}]/[X_t], \quad (6)$$

sorbed Me^{2+} and X_t are in mol/g, and $N_{CaX} = 1\text{-}N_{MeX}$. Equation (5) is a log transformation of the empirical power exchange function described by LANGMUIR (1981) for the homovalent binary surface exchange of aqueous species A (i.e., Me) for species B (i.e., Ca) on the sorbent:

$$K_{ex} = \frac{(B)}{(A)}\left[\frac{N_{AX}}{N_{BX}}\right]^n \quad (7)$$

where n is an empirical constant and K_{ex} is the exchange constant of the reaction. If the isotherm exhibits unit slope on a log-log plot (i.e., $n = 1$), then the exchange reaction may be considered ideal (see SPOSITO and MATTIGOD, 1979) and the power exchange function becomes identical to the equilibrium quotient for the conditional equilibrium constant ${}^cK_{ex}$:

$${}^cK_{ex} = (B)[N_{AX}]/(A)[N_{BX}]. \quad (8)$$

The applicability of the power exchange isotherm to Zn sorption on calcite has been described by ZACHARA et al. (1988).

The speciated aqueous equilibrium concentrations were also used to calculate ion activity products for Me^{2+} solid phases that have rapid precipitation/dissolution kinetics at room temperature and pressure and could conceivably precipitate in the sorption experiments (Appendix Table III). The equilibrium isotherm solutions that computed to be saturated with these phases are marked on Fig. 4b. Precipitation of solid phases occurred for all of the metals at the highest initial Me^{2+} concentrations (10^{-5} to 10^{-4} mol/L). Invariably, the equilibrium solutions computed to be saturated with discrete solid phases when the isotherms displayed either a positive or negative change in slope (Fig. 4a, 4b).

Where discrete solid phase precipitation did not occur, the exchange isotherms for Ni, Co, Mn, and Cd were nearly parallel. The slope of these isotherms was approximately 1, signifying that a single exchange constant could describe the sorption/surface reaction (i.e., $n = 1$ in Eqns. 5 and 7). The two different Zn isotherms at pH 7.4 and 8.4 in Fig. 4a defined an identical exchange isotherm in Fig. 4b after accounting for the effects of hydrolysis, aqueous complexation, and Ca^{2+} concentration. Similarly, ZACHARA et al. (1988) observed that Zn isotherms measured over a range in CO_2 partial pressures and pH also defined a single exchange function similar to that in Fig. 4b. The exchange function of ZACHARA et al. (1988) was identical to that in Fig. 4b if differences in the surface Ca concentrations as measured by isotopic exchange were taken in account. The Zn isotherms differed from the other sorbates and exhibited a high exponential term (i.e., $n = 1.86$ in Eqn. 5). The selectivity sequence of the speciated exchange isotherms in Fig. 4b, Cd > Zn > Mn > Co > Ni, was comparable to that observed for the sorption edges (Fig. 2a). It was evident from Fig. 4b that the selectivity difference between Zn and the other metals was a strong function of sorption density (i.e., $[N_{MeX}/N_{CaX}]$).

Sorption Modelling

Half-reaction exchange constants for each of the metal ions on cation specific sites (X) on the surface of calcite were determined using the data in Fig. 2a, the FITEQL program (WESTALL, 1982a,b), and the solution composition data and complexation reactions summarized in Appendix Tables I and II. The averaged value of $Ca_{(s)}$ derived from the isotopic exchange data was assumed to equal the total number of cation specific surface sites (X_t). It should be noted, however, that limited data suggests that only 10% or less of the surface sites estimated by isotopic exchange on calcite may actually be accessible to minor ion sorbates (ZACHARA et al., 1988; COWAN et al., 1990).

The half reactions for Ca and metal ion exchange on calcite were

$$(Ca^{2+})aq + X = X\text{-Ca} \quad K_{Ca} \quad (9)$$

and

$$(Me^{2+})aq + X = X\text{-}Me \quad K_{Me} \qquad (10)$$

where ( ) signifies single-ion activity. To initialize the modelling calculation, the half-reaction constant for Ca was fixed at high value (log K_{Ca} = 15) to ensure that all the cation-specific surface sites (X_t) were occupied by Ca before metal sorption commenced. Surface saturation with Ca is consistent with electrokinetic measurements on calcite (THOMPSON and POWNALL, 1989). The half-reaction constant for the metal was determined by fitting to the fractional sorption data versus pH in Fig. 2a. The overall exchange constant $^cK_{ex}$ for the surface reaction

$$X\text{-}Ca + (Me^{2+})aq = X\text{-}Me + (Ca^{2+})aq \qquad (11)$$

was calculated from the difference in the half-reaction constants; i.e., log $^cK_{ex}$ = log K_{Me} − log K_{Ca}. The surface exchange constant ($^cK_{ex}$) was conditional (denoted by c) in that surface concentrations (in mol/L) rather than surface activities were used in the reaction quotient. This $^cK_{ex}$ is similar to the Vanselow exchange constant (K_V) used in modelling of Mn^{2+} sorption to siderite (WERSIN et al., 1989). As discussed previously for Eqn. (4), Eqn. (11) embodies no assumption, implicit or explicit, regarding the chemical nature of the surface species, X-Me. The surface species may be a surface complex between the hydrated metal ion and a structurally bound carbonate ion (as hypothesized for Zn, Co, and Ni) or a dehydrated surface phase of uncertain molecular properties (as presumed for Mn and Cd). Exchange reactions such as Eqn. (11) have been used to describe different reactions ranging from adsorption to precipitation, including ion exchange on layer silicates (SHAVIV and MATTIGOD, 1985; FLETCHER and SPOSITO, 1989) and solid solution formation in carbonates (MCINTIRE, 1963; SPOSITO, 1981; DAVIS et al., 1987).

The sorption edges for all metals in Fig. 2a, except Ni, could be quantitatively described with a single exchange reaction between X-Ca and the uncomplexed divalent metal cation Me^{2+} (Fig. 5a and b). Constants describing the divalent metal ion surface exchange ($^cK_{ex}$) are summarized in Table 1. Sorption edges for Cd and Mn could also be quantitatively described by an exchange reaction between Me^{2+} and surface Ca, in spite of their limited sorption reversibility (modelling not shown). The decrease in the sorption of Co^{2+} above pH 8.5 (Fig. 2a) could only be simulated by including the aqueous species $Co(CO_3)_2^{2-}$ (Fig. 5b). A constant was estimated for this complex (log K = 7.46) while fitting an exchange constant for Co^{2+} to the sorption data in Fig. 2a. The existence of ML_2-type carbonate complexes for Cu was suggested by SCHINDLER et al. (1968), and a similar complex may exist for Co, because Cu^{2+} and Co^{2+} have identical ionic radii (0.72 Å). The fitted value for the log K of $Co(CO_3)_2^{2-}$ was similar in magnitude to stability constants for ML_2-type complexes of other divalent metallic cations estimated by MATTIGOD and SPOSITO (1977).

In contrast to the other metals, a second surface complex (X-NiOH) in addition to X-Ni was required to quantitatively describe the sorption edge of Ni on calcite (Fig. 6a). The increase in Ni sorption above pH 8.7 (Fig. 6a) could not be described with X-Ni alone, because at and above that pH,

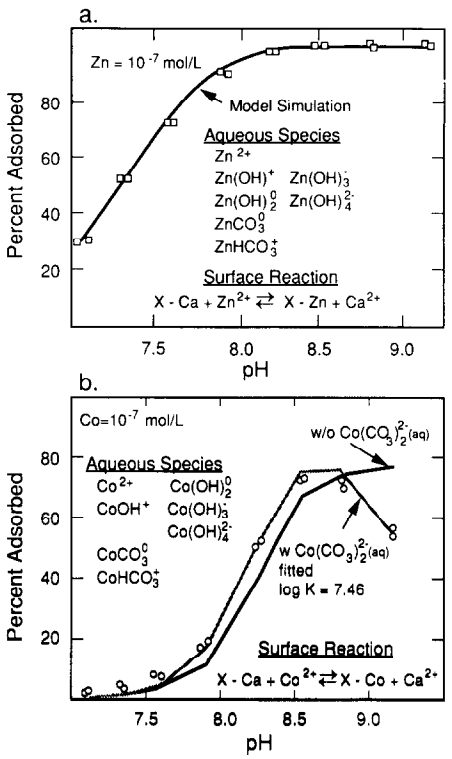

FIG. 5. Half-reaction exchange modeling of Zn and Co sorption on calcite over a range in Ca^{2+} concentration. Aqueous and surface species are as noted. Sorption data is from Fig. 2, and both solid and textured lines are model calculations.

aqueous Ni was calculated to exist primarily as hydrolyzed species [$NiOH^+$ and $Ni(OH)_2^0$] and the carbonate complex $NiCO_3^0$(aq). The hydrolyzed surface species (X-NiOH) was therefore calculated to be important above pH 8.5 (Fig. 6a) and was calculated to be more strongly bound than the divalent metal cation (e.g., log $^cK_{ex}$(Ni) = 0.51 and log $^cK_{ex}$(NiOH) = 1.06). If, however, the log formation constant for the $NiCO_3^0$(aq) was reduced from 4.83 (Appendix Table II) to a fitted value of 4.37, the Ni sorption edge (Fig. 2a) could be quantitatively described using only the divalent cation complex (X-Ni) (Fig. 6b).

Because the calculated distribution of surface complexes and the value of the exchange constants for Ni varied with the magnitude of the log $K[NiCO_3^0(aq)]$, a sensitivity analysis was performed for Cd, Co, Ni, and Zn (Table 2) to determine the potential for variability in the log $^cK_{ex}$ of X-Me given the range in measured and estimated literature values for log $K[MeCO_3^0(aq)]$. As shown in Table 2, using different literature values for log $K[MeCO_3^0(aq)]$ did not cause significant variability in the surface exchange constants for Cd^{2+} and Zn^{2+}. For Co and Ni, whose literature values for log $K[MeCO_3(aq)]$ varied by factors of 10 or greater, the variability was more significant. Nickel showed the greatest variation. The final set of exchange constants for X-Me, which were based on the complexation constants in Appendix Table II, are summarized in Table 1.

The surface exchange constants in Table 1 combined with the complexation constants in Appendix Table II provided

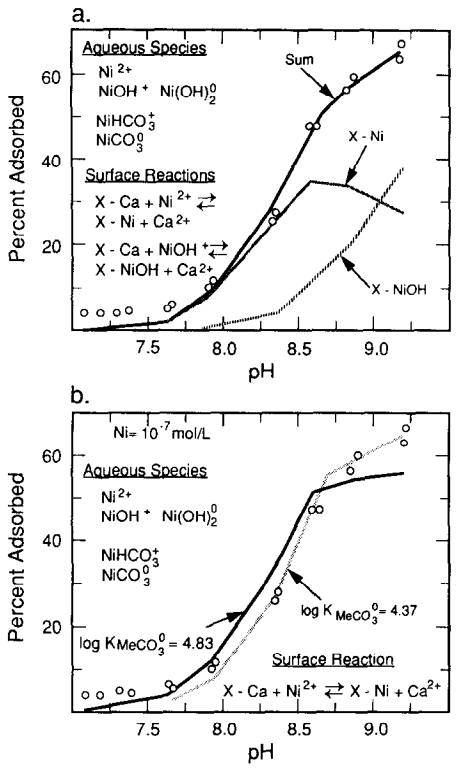

FIG. 6. Half-reaction exchange modeling of Ni on calcite over a range in Ca^{2+} concentration: (a) modeling with X-Ni and X-NiOH surface species and (b) modeling with best fit $K_{MeCO_{3(aq)}}$. Aqueous and surface species are as noted. Sorption data is from Fig. 2; both solid and textured lines are model calculations.

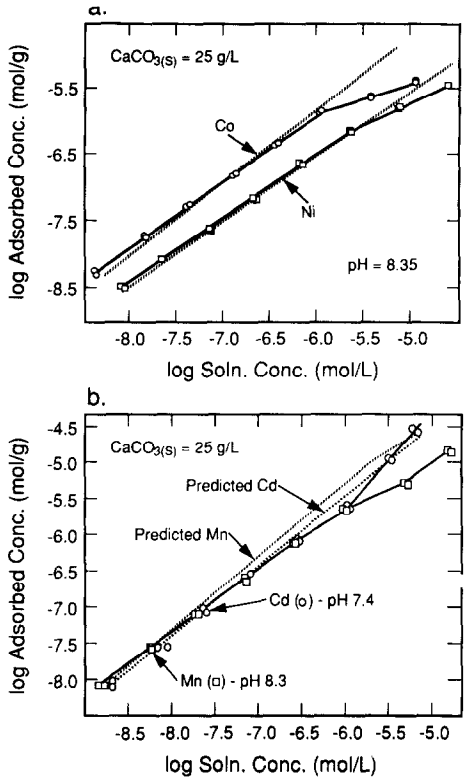

FIG. 7. Agreement between predicted isotherms and isotherm experimental data from Fig. 4a. Dotted lines are model predictions. Half-reaction exchange constants are derived from Fig. 2 and are summarized in Table 1.

predictions of the sorption isotherms in Fig. 4a that varied in their agreement with the experimental data (Fig. 7). Agreement was best (Fig. 7) for those metals exhibiting a slope of near unity on the exchange isotherm plots of Fig. 4b (e.g., Ni, Co, and Cd). Deviation of the predicted isotherm from the experimental data was greatest when discrete phase precipitation occurred (e.g., Co at solution concentrations greater than 10^{-6} mol/L and Ni at solution concentration greater than $10^{-5.5}$ mol/L; Fig. 7a). In general, however, the exchange constant for the single X-Me surface complex provided good predictions of the sorption of Ni, Co, Cd, and Mn over a range of three orders of magnitude in surface coverage, until discrete solid phase precipitation of $MeCO_3(s)$ or $Me(OH)_2(s)$ occurred.

Table 2. Sensitivity calculation to determine effect of $K_{MeCO3(aq)}$[a] on $^cK_{ex}$[b]

Metal	Log $K_{MeCO3(aq)}$	Log $^cK_{ex}$
Cd	5.40	3.03
	2.42	3.02
Co	4.91	0.79
	2.55	0.44
Ni	6.87	2.08
	2.56	-0.11
Zn	6.63	2.89
	2.55	2.43

a Based on range of $K_{MeCO3(aq)}$ reported in FOUILLAC and CRIAUD (1984), Table 2.
b $^cK_{ex}$ as defined in Table 1.

A single exchange constant could not adequately predict the placement of the Zn isotherms (not shown), because of their nonlinearity (e.g., slope of 1.86 on Fig. 4b). No explanation accounted for this anomalous isotherm behavior of Zn. The isotherm data implied that sites on the calcite surface exhibit heterogeneity in their binding energy with Zn. Log exchange constants (log $^cK_{ex}$) varying from approximately 3.0 to 1.5 were required to describe the Zn isotherm.

Correlations and Significance of Exchange Constants

The X-Me exchange constants ($^cK_{ex}$, Table 1) were not uniformly correlated with any single property of the metallic cations. The exchange constants decreased sharply as r_x of the metal ion exceeded that of Ca (Fig. 8a), suggesting that ion size influences sorptivity on calcite. Metals with ionic radii greater than Ca (i.e., Ba and Sr) form orthorhombic anhydrous carbonates (aragonite structure), because their larger size is incompatible with the octahedral coordination environment in the rhombohedral structure of calcite (REEDER, 1983). The exchange constants for the metals with

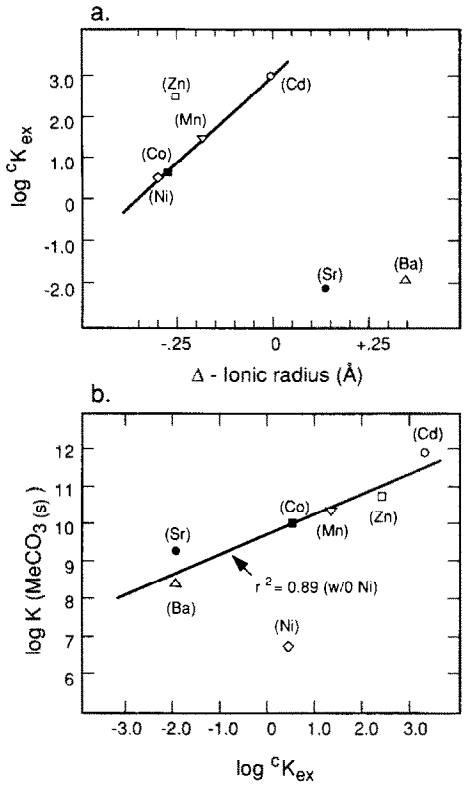

FIG. 8. Relationship between MeX surface-exchange constants and (a) difference in ionic radius between Me^{2+} and Ca^{2+} and (b) solubility product of the anhydrous metal carbonate, $MeCO_3(s)$. Values for Ba and Sr are orthorhombic carbonates; all others are rhombohedral carbonates.

smaller r_x than Ca increased as their ionic radii approached Ca (Fig. 8a), suggesting that the cation whose size was closest to the structural cation was preferred on the surface. Zinc was anomalous with respect to this size trend (Fig. 8a), implying that other factors perhaps related to the electronic environment of the metallic cation were also important. The exchange constants for all the metals except Ni were found to correlate well with the solubility of the anhydrous metal carbonate solid ($MeCO_3(s)$) (Fig. 8b). The trend in Fig. 8b circumstantially suggests that the equilibrium constant for $NiCO_3(s)$ may be in error. Similarly, the selectivity of metal cation adsorption on geothite (α-FeOOH), where the surface complex is strong and believed to be inner sphere (DAVIS and KENT, 1990), correlated with the solubilities of the individual metal hydroxides (GRIMME, 1969). Correlations between the metal exchange constants and any of the aqueous complexation constants for carbonate or bicarbonate complexes (i.e., $MeCO_3^0(aq)$) were poor. The good correlation between $^cK_{ex}$ and $K(MeCO_{3(s)})$ indicates that direct chemical, rather than electrostatic, interaction controls the binding strength of the sorbing metallic cations with the calcite surface.

The present data cannot resolve whether the exchange reaction occurs on or within a partially hydrated layer on the calcite surface (e.g., DAVIS et al., 1987) or within a structural surface site with 3- to 5-fold coordination (e.g., REEDER and PROSKY, 1986; REEDER and GRANS, 1987). We note, however, that the metal-ion selectivity sequence in Figs. 2 and 4 is opposite to that proposed for metal ion incorporation into structural protosites (REEDER and GRANS, 1987), where the smallest ion is thought to be preferred. Regardless of the location of the metal binding sites on the surface of calcite, the correlations in Fig. 8 imply that metal binding sites exhibit structural organization and uniformity because they apparently demonstrate discrete preference and chemical selectivity based on the electronic properties of the sorbing metals. The unit isotherm slopes for Co and Ni and the constant conditional-exchange constants ($^cK_{ex}$) observed for these metals over a range in surface coverage suggest that the surface sites have uniform sorption energies. The contrasting heterogenous behavior of Zn was anomalous and unexplainable.

Relationship to Surface Precipitation

Two models involving coupled adsorption/precipitation processes have been proposed to describe the sorption behavior of metal ions on carbonate surfaces (DAVIS et al., 1987; COMANS and MIDDELBURG, 1987). Both models postulate that the metal ions first bind to the calcite surface through an adsorption reaction and then dehydrate to yield a surface co-precipitate, termed a solid solution by both authors. The models differ, however, in their conceptual view of the co-precipitation reaction. In the model of DAVIS et al. (1987), the formation of co-precipitate can occur at any surface loading, whereas in the model of COMANS and MIDDLEBURG (1987) co-precipitation commences only when surface adsorption sites become saturated. While the present study has emphasized the initial adsorption reaction, the multi-metal sorption data in this paper allows comment on the veracity of these models and the nature of the surface precipitation reaction.

Two patterns of Me surface precipitation are evident in this paper and publications by MCBRIDE (1979), DAVIS et al. (1987), and ZACHARA et al. (1989). The first pattern is consistent in general aspects with the model of DAVIS et al. (1987) and is represented by the sorption data for Mn and Cd. These two metal ions appear to dehydrate rapidly after being adsorbed, forming a surface phase at low fractional occupancy (<1%) of surface sites. Data is not available to determine whether the surface phase exhibits two-dimensional (i.e., the surface solid solution of MCBRIDE, 1979) or three-dimensional molecular arrangement, (i.e., the solid solution of DAVIS et al., 1987), criteria necessary to define the nature of the surface phase (SPOSITO, 1986). The second pattern of surface precipitation is represented by the present sorption data for Co, Ni, and Zn and is only partially consistent with either the model of DAVIS et al. (1987) or that of COMANS and MIDDELBURG (1987). These latter metal ions do not appear to form surface co-precipitates, but rather appear to persist on the calcite surface as hydrated complexes until they are either incorporated into the lattice by recrystallization, or aqueous Me concentrations exceed the solubility product of and induce precipitation of discrete Me solids with rapid precipitation kinetics (e.g., see Fig. 4b and ZACHARA et al., 1989).

The arguments immediately above are based on speculation that metals that are desorbable from calcite (i.e., Zn, Ni, and Co) exist as hydrated adsorbed species on the surface or

within the surface layer. The distinction between adsorbed and precipitated species, however, is difficult to resolve at low surface concentrations inaccessible with spectroscopy (see SPOSITO, 1986). The ambiguity between precipitation and adsorption for metallic cations on calcite is highlighted in Table 3, where the surface exchange constants (${}^{c}K_{ex}$) for *X*-Me surface complexes (Table I) are compared to solid phase distribution coefficients, *D* (as defined by MCINTIRE 1963), that describe Me partitioning into surface layers on calcite (d and e) or calcite co-precipitates (a–c, f–i, g–k). Solid phase distribution coefficients often are dependent on precipitation rate (LORENS, 1981; LAHANN and SIEBERT, 1982; PINGATORE and EASTMAN, 1986; PINGATORE et al., 1988), and the ranges for D reported in Table 3 reflect these rate dependencies. In general, however, the surface exchange constants follow the same trend as and are similar in magnitude to the distribution coefficients, despite their being measured and calculated differently. This similarity suggests that the same chemical factors control the magnitude of both ${}^{c}K_{ex}$ and *D*. Given the relationship observed in Fig. 8b, this similarity would be expected, because *D* is also related to the solubility of the anhydrous carbonate ($D = K_{CaCO_{3(s)}}/K_{MeCO_{3(s)}}$ if the solid solution is ideal; MCINTIRE, 1963).

SUMMARY

Divalent metals sorb to calcite according to the selectivity sequence Cd > Zn ≥ Mn > Co > Ni ≫ Ba = Sr. Desorption was found to correlate with the hydration energy of the metals; ions with the highest hydration energies were most desorbable. The magnitude of sorption depended on the aqueous Ca concentration, and sorption could be described as a surface exchange reaction between Me^{2+} and Ca^{2+} ions on cation-specific surface sites (*X*). The sorption model presumed no explicit molecular form for the surface complex (*X*-Me), because the form is not known with certainty and appears to differ between metals. Exchange constants for the *X*-Me surface complex (i) correlated, in part, with the ionic radius of the metal sorbates and the solubility products of $MeCO_3(s)$ solids and (ii) were similar in magnitude and in trend to solid phase distribution coefficients for these metals in calcite co-precipitates and overgrowths.

Our data for Cd and Mn were consistent in trend with the model of DAVIS et al. (1987), where the adsorbed metals dehydrate on the calcite surface, forming a phase that behaved as a surface precipitate. The macroscopic sorption data, however, could not resolve whether this surface phase was a two- or three-dimensional co-precipitate. Therefore, a rigorious assessment of the surface reaction sequence proposed by DAVIS et al. (1987) was not possible. In contrast, Zn, Co, and Ni appeared in our study to remain on the calcite surface as hydrated complexes until (i) they were incorporated into the calcite structure by recrystallization or (ii) aqueous Me concentrations maintained by the surface-exchange reaction exceeded the ion activity product of $Zn_5(OH)_6(CO_3)_2(s)$, $Co(OH)_2(s)$, or $Ni(OH)_2(s)$ allowing for their heterogeneous

Table 3. Surface exchange constants (${}^{c}K_{ex}$) and reported solid phase distribution coefficients (D)

Metal	Log ${}^{c}K_{ex}$ (X-Me)	Log D and Sources
Ba	-1.93	-1.22[a]
Sr	-2.04	-1.30[a], -0.69 to -1.22[b], -.52[c]
Cd	3.02	3.17[d], ~1.46[e]
Mn	1.31	0.6-1.39[f], 1.35[e], 0-1.25[g], 1.24[h], 1.17[i], 0.73[j]
Zn	1.43	>1.75[k], 0.75-1.31[l]
Co	0.56	0.68[e]
Ni	0.51	

a PINGITORE and EASTMAN (1984)
b PINGITORE and EASTMAN (1986)
c MUCCI (1986), average log D with Ω=1.8 to 14.4
d DAVIS *et al.* (1987), log D in surface layer
e LORENS (1981), log D at 0 rate
f MCBRIDE (1979), log D in surface layer
g PINGITORE *et al.* (1988)
h STUMM and MORGAN (1981)
i BODINE *et al.* (1965)
j MICHARD (1968)
k TSUSUE and HOLLAND (1966)
l GLASNER and WEISS (1980)

$$D = \text{solid phase distribution coefficient} = \frac{X_{Me}/X_{Ca}}{[Me^{2+}]/[Ca^{2+}]}$$

where X is mole fraction and [ ] is aqueous concentration

precipitation. Observations herein do not support the surface precipitation model for calcite proposed by COMANS and MIDDELBURG (1987), but our data were not sufficient for performing comprehensive evaluation.

The magnitude of sorption on calcite for many of the metals (Cd, Mn, Zn, Co, and possibly Ni) was sufficiently large to imply that calcite could act as an important sorbent for metals in calcareous soils and groundwater. An approximate calcite surface area of only 0.0017 m^2/g is required in a water-saturated aquifer material of 50% porosity to yield the same fractional of sorption as shown in Figs. 2a and 4. Sensitivity calculations on hypothetical aquifer materials containing calcite, layer silicates, and amorphous Fe-oxide (ZACHARA et al., 1990) also attest to the potential importance of calcite as a metal sorbent in aquifer materials. The extent of sorption reversibility on calcite, however, has important ramifications for metal ion transport in calcareous systems. The limited desorption of Cd and Mn from calcite suggests that sorption may be irreversible for these ions over the temporal scale of water movement in soils and aquifers. While sorption reactions for Zn, Co, and Ni appear mostly reversible, nonequilibrium sorption behavior could become evident in natural systems as a result of calcite recrystallization.

Acknowledgments—This research was supported by the Ecological Research Division (ERD), Office of Health and Environmental Research (OHER), US Department of Energy, under Contract DE-AC06-76RLO 1830 as part of OHER's Subsurface Science Program. The continued support of Dr. F. J. Wobber and ERD is appreciated.

Editorial handling: E. J. Reardon

REFERENCES

BAES C. F. and MESMER R. E. (1976) *The Hydrolysis of Cations*. J. Wiley & Sons.

BALL J. W., NORDSTROM D. K., and JENNE E. A. (1981) Additional and revised thermochemical data and computer code for WATEQ2—A computerized chemical model for trace and major element speciation and mineral equilibria of natural waters. *WRI 78-116*. US Geological Survey, Menlo Park, CA.

BILINSKI H., HUSTON R., and STUMM W. (1976) Determination of the stability constants of some hydroxo carbonato complexes of Pb(II), Cu(II), Cd(II), and Zn(II) in dilute solutions by anodic stripping volammetry and differential pulse polarography. *Anal. Chim. Acta* **84,** 157–164.

BODINE M. W., HOLLAND H. D., and BORCSIK M. (1965) Coprecipitation of manganese and strontium with calcite. In *Problems of Postmagmatic Ore Deposition*. Vol. 2, pp. 401–405. Geol. Surv. Czeh., Prague.

BURGESS J. (1978) *Metal Ions in Solution*. Ellis Horwood Ltd.

COMANS R. N. and MIDDELBURG J. J. (1987) Sorption of trace metals by calcite: Applicability of the surface precipitation model. *Geochim. Cosmochim. Acta* **51,** 2587–2591.

COREY R. B. (1981) Adsorption vs. precipitation. In *Adsorption of Inorganics at Solid-Liquid Interfaces* (eds. M. A. ANDERSON and A. J. RUBIN), pp. 161–182. Ann Arbor Science, Ann Arbor, MI.

COSOVIC B., DEGOBBIS D., BILINSKI H., and BRANICA M. (1982) Inorganic cobalt species in seawater. *Geochim. Cosmochim. Acta* **46,** 151–158.

COWAN C. E., ZACHARA J. M., and RESCH C. T. (1990) Solution ion effects on the surface exchange of selinite on calcite. *Geochim. Cosmochim. Acta* **54,** 2223–2234.

DAVIS J. A. and KENT D. B. (1990) Surface Complexation Modeling in Aqueous Geochemistry. In *Mineral-Water Interface Geochemistry* (eds. M. F. HOCHELLA JR. and A. F. WHITE); *Reviews in Mineralogy 23*, pp. 177–260. Mineralogical Society of America.

DAVIS J. A., FULLER C. C., and COOK A. D. (1987) A model for trace metal sorption processes at the calcite surface: Adsorption of Cd^{2+} and subsequent solid solution formation. *Geochim. Cosmochim. Acta* **51,** 1477–1490.

DUDLEY L. M., MCLEAN J. E., SIMS R. C., and JURINAK J. J. (1988) Sorption of copper and cadmium from the water soluble fraction of an acid mine waste by two calcareous soils. *Soil Sci.* **145,** 207–214.

FELMY A. R., GIRVIN D. C., and JENNE E. A. (1984) *MINTEQ*. A computer model for calculating aqueous geochemical equilibria. *NTIS-PB-84157148*. Natl. Tech. Information Service.

FLETCHER P. and SPOSITO G. (1989) The chemical modelling of clay/electrolyte interactions for montmorillonite. *Clay Mineral.* **24,** 375–391.

FOUILLAC C. and CRIAUD A. (1984) Carbonate and bicarbonate trace metal complexes: Critical re-evaluation of stability constants. *Geochem. J.* **18,** 297–303.

FOXALL T., PETERSON G., RENDALL H. M., and SMITH A. L. (1979) Charge determination at the calcium salt/aqueous solution interface. *J. Chem. Soc., Faraday Trans. I.* **75,** 1034–1039.

FRANKLIN M. L. and MORSE J. W. (1983) The interaction of manganese(II) with the surface of calcite in dilute solutions and seawater. *Mar. Chem.* **12,** 241–254.

FULLER C. C. and DAVIS J. A. (1987) Processes and kinetics of Cd^{2+} sorption by a calcareous aquifer sand. *Geochim. Cosmochim. Acta* **51,** 1491–502.

GLASNER A. and WEISS D. (1980) The crystallization of calcite from aqueous solutions and the role of zinc and magnesium ions. I. Precipitation of calcite in the presence of Zn^{2+} ions. *J. Inorg. Nucl. Chem.* **42,** 655–663.

GRIMME H. (1969) Die Adsorption ion Mn, Co, Cu, and Zn, Durch Goethite Aus Verdunnten Losungen. Z. Pflanzenernahi. *Dung Bodenkunde* **121,** 58–65.

HOCHELLA M. F. (1990) Atomic Structure, Microtopography, Composition, and Reactivity of Mineral Surfaces. In *Mineral-Water Interface Geochemistry* (eds. M. F. HOCHELLA JR. and A. F. WHITE); *Reviews in Mineralogy 23*, pp. 87–132. American Mineralogical Society.

INKS C. G. and HAHN R. B. (1967) Determination of surface area of calcium carbonate by isotopic exchange. *Anal. Chem.* **39,** 625–628.

JOHNSON K. S. (1982) Solubility of rhodochrosite ($MNCO_3$) in water and seawater. *Geochim. Cosmochim. Acta* **46,** 1805–1809.

KAUSHANSKY P. and YARIV S. (1986) The interactions between calcite particles and aqueous solutions of magnesium, barium or zinc chlorides. *Appl. Geochem.* **1,** 607–618.

KORNICKER W. A., MORSE J. W., and DAMASCENOS R. N. (1985) The chemistry of Co^{2+} interaction with calcite and aragonite surfaces. *Chem. Geol.* **53,** 229–236.

KOSS V. and MOLLER P. (1974) Surface ion exchange on calcite powder in the presence of Mn^{2+} ions. *Inorg. Nucl. Chem. Lett.* **10,** 849–854.

KUKURA M., BELL L. C., POSNER A. M., and QUIRK J. P. (1972) Radioisotopic determination of the surface concentrations of calcium and phosphorous on hydroxyapatite in aqueous solution. *J. Phys. Chem.* **76,** 900–905.

LAHANN R. W. and SIEBERT R. M. (1982) A kinetic model for distribution coefficients and application to Mg calcites. *Geochim. Cosmochim. Acta* **46,** 2229–2237.

LANGMIUR D. (1981) The power exchange function: A general model for metal adsorption onto geologic materials. In *Adsorption from Aqueous Solutions* (ed. P. H. TEWARI), pp. 1–18. Plenum Press.

LESHT D. and BAUMAN J. E. (1978) Thermodynamics of the manganese (II) bicarbonate system. *Inorg. Chem.* **17,** 3332–3336.

LIPPMANN F. (1973) *Sedimentary Carbonate Minerals*. Springer-Verlag, Berlin.

LORENS R. B. (1981) Sr, Cd, Mn, and Co distribution coefficients in calcite as a function of calcite precipitation rate. *Geochim. Cosmochim. Acta* **45,** 553–561.

MATTIGOD S. V. and SPOSITO G. (1977) Estimated association constants for some complexes of trace metals with inorganic ligands. *Soil Sci. Soc. Amer. J.* **41,** 1092–1097.

McBRIDE M. B. (1979) Chemisorption and precipitation of Mn^{2+} at $CaCO_3$ surfaces. *Soil Sci. Soc. Amer. J.* **41,** 693–698.

McBRIDE M. B. (1980) Chemisorption of Cd^{2+} on calcite surfaces. *Soil Sci. Soc. Amer. J.* **44,** 26–28.

McINTIRE W. L. (1963) Trace element partition coefficients—A review of theory and application to geology. *Geochim. Cosmochim. Acta* **27,** 1209–1264.

MICHARD G. (1968) Coprecipitation de l'ion manganeaux avec le carbonate de calcium. *C. R. Acad. Sci., Paris, Ser. D* **267,** 1685–1688.

MOLLER P. (1973) Determination of the composition of surface layers of calcite in solutions containing Mg^{2+}. *J. Inorg. Nucl. Chem.* **35,** 395–401.

MOLLER P. and SASTRI C. S. (1974) Estimation of the number of surface layers of calcite involved in Ca^{45} Ca isotopic exchange with solution. *Z Phys. K. Chem. Folge.* **89,** 80–87.

MORSE J. W. (1986) The surface chemistry of calcium carbonate minerals in natural waters: An overview. *Mar. Chem.* **20,** 91–112.

MOZETO A. A., FRITZ P., and REARDON E. J. (1984) Experimental observations on carbon isotope exchange in carbonate-water systems. *Geochim. Cosmochim. Acta* **48,** 495–504.

MUCCI A. (1986) Growth kinetics and composition of magnesium calcite overgrowths precipitated from seawater: Quantitative influence of orthophosphate ions. *Geochim. Cosmochim Acta* **50,** 2255–2265.

MUCCI A. and MORSE J. W. (1983) The incorporation of Mg^{2+} and Sr^{2+} into calcite overgrowths: Influences of growth rate and solution composition. *Geochim. Cosmochim. Acta* **47,** 217–233.

NAUMOV G. B., RYZHENKO B. N., and KHODAKOVSKY I. L. (1974) *Handbook of Thermodynamic Data.* USGS WRD-74-001, NTSS Document PB 226 722.

PAPADOPOULOS P. and ROWELL D. L. (1988) The reaction of cadmium with calcium carbonate surfaces. *J. Soil Sci.* **39,** 23–36.

PINGITORE N. E. and EASTMANN M. P. (1984) The experimental partitioning of Ba^{2+} into calcite. *Chem. Geol.* **45,** 113–120.

PINGITORE N. E. and EASTMAN M. P. (1986) The coprecipitation of Sr^{2+} with calcite at 25°C and 1 atm. *Geochim. Cosmochim. Acta* **50,** 2195–2203.

PINGITORE N. E., EASTMAN M. P., SANDIDGE M., ODEN K., and FREIHA B. (1988) The coprecipitation of manganese (II) with calcite: An experimental study. *Mar. Chem.* **25,** 107–120.

PLUMMER L. N. and BUSENBERG E. (1987) Thermodynamics of aragonite-strontianite solid solutions: Results from stoichiometric solubility at 25 and 76°C. *Geochim. Cosmochim. Acta* **51,** 1393–1411.

RAI D., FELMY A. R., and MOORE D. A. (1991) An aqueous thermodynamic model for Cd^{2+}-CO_3^{2-} interaction in high ionic strength carbonate solutions, and the solubility product of $CdCO_3$(s). *Inorg. Chem.* (in press).

REDDY M. M. and NANCOLLAS G. R. (1971) The crystallization of calcium carbonate 1. Isotopic exchange and kinetics. *J. Colloid. Inter. Sci.* **36,** 166–173.

REEDER R. J. (1983) Crystal chemistry of the rhombohedral carbonates. In *Carbonates: Mineralogy and Chemistry* (ed. R. J. REEDER); *Reviews in Mineralogy II.* Mineralogical Society of America.

REEDER R. and GRANS J. C. (1987) Sector zoning in calcite cement crystals: Implications for trace element distributions in carbonates. *Geochim. Cosmochim. Acta* **51,** 187–194.

REEDER R. and PROSKY J. L. (1986) Compositional sector zoning in dolomite. *J. Sediment. Petrol.* **56,** 237–247.

RYAN M. P. and BAUMAN J. E. (1978) Thermodynamics of the zinc bicarbonate ion pair. *Inorg. Chem.* **17,** 3329–3332.

SASTRI C. S. and MOLLER P. (1974) Study of the influence of Mg^{2+} ions on the Ca-Ca^{-45} isotopic exchange on the surface layers of calcite single crystals. *Chem. Phys. Lett.* **26,** 116–120.

SCHINDLER P., REINERT M., and GAMSJAGER H. (1968) Loklichkeitkonstanten und freie bildungsenthalipie von $Cu_2(OH)_2CO_3$ (Malachit) und $Cu_3(OH)_2(CO_3)_2$ (Azurit) bei 25°C. *Helv. Chim. Acta* **51,** 1845–1856.

SHAVIV A. and MATTIGOD S. V. (1985). Cation exchange equilibria expressed as a cation-ligand complex formation. *Soil Sci. Soc. Amer. J.* **49,** 569–573.

SMITH R. M. and MARTELL A. E. (1976). *Critical Stability Constants, Vol. 4: Inorganic Complexes.* Plenum Press, New York.

SPOSITO G. (1986) Distinguishing adsorption from surface precipitation. In *Geochemical Processes of Mineral Surfaces* (eds. J. A. DAVIS and K. F. HAYES); *ACS Symposium Series 323,* pp. 217–228.

SPOSITO G. and MATTIGOD S. V. (1979) Ideal behavior in Na^+-trace metal cation exchange on Camp Berteau montmorillonite. *Clays Clay Mineral.* **27,** 125–128.

SPOSITO G. (1981) *The Thermodynamics of Soil Solutions.* Oxford University Press.

STIPP S. and HOCHELLA M. F., JR. (1991) Structure and bonding environments at the calcite surface as observed by x-ray photoelectron spectroscopy (XPS) and low energy electron diffraction (LEED). *Geochim. Cosmochim. Acta* (in press).

STUMM W. and MORGAN J. J. (1981). *Aquatic Chemistry.* J. Wiley & Sons.

THOMPSON D. W. and POWNALL P. G. (1989) Surface electrical properties of calcite. *J. Colloid. Inter. Sci.* **131,** 74–82.

TSUSUE A. and HOLLAND H. D. (1966) The coprecipitation of cations with $CaCO_3$—III. The coprecipitation of Zn^{2+} with calcite between 50 and 250°C. *Geochim. Cosmochim. Acta* **30,** 439–453.

WAGMAN D., EVANS W. H., PARKER V. B., SCHUMM R. H., HALOW I., BAILEY S. M., CHURNEY K. L., and NUTTALL R. L. (1982) The NBS tables of chemical thermodynamic properties: Selected values for inorganic and C_1 and C_2 organic substances in SI units. *J. Phys. Chem. Ref. Data 11: Suppl 2.*

WERSIN P., CHARLET L., KARTHEIN R., and STUMM W. (1989) From adsorption to precipitation: Sorption of Mn^{2+} on $FeCO_3$(s). *Geochim. Cosmochim. Acta* **53,** 2787–2796.

WESTALL J. (1982a) FITEQL, A computer program for determination of equilibrium constants from experimental data. Version 1.2. Report 82-01, Department of Chemistry, Oregon State University, Corvallis, Oregon.

WESTALL J. (1982b) FITEQL, A computer program for determination of equilibrium constants from experimental data. Version 2.0. Report 82-02, Department of Chemistry, Oregon State University, Corvallis, Oregon.

ZACHARA J. M., KITTRICK J. A., and HARSH J. B. (1988) The mechanism of Zn^{2+} adsorption on calcite. *Geochim. Cosmochim. Acta* **52,** 2281–2291.

ZACHARA J. M., KITTRICK J. A., and HARSH J. B. (1989). Solubility and surface spectroscopy of zinc precipitates on calcite. *Geochim. Cosmochim. Acta* **53,** 9–19.

ZACHARA J. M., COWAN C. E., and RESCH C. T. (1990). Metal cation/anion adsorption on calcium carbonate: Implications to metal ion concentrations in groundwater. In *Proceedings of EPA Workshop on Metal Speciation and Transport in Groundwaters. Jekyll Island, Georgia. May 24–26, 1989* (eds. M. PURDUE and H. ALLEN).

ZHOROV V. A., BEZBORODOV A. A., and POPOV N. I. (1976). Predominance area diagrams and equilibrium ratios of inorganic forms of cobalt and nickel in oceanic water. *Oceanol.* **16,** 808–814.

ZULLIG J. J. and MORSE J. W. (1988) Interaction of organic acids with carbonate mineral surfaces in seawater and related solutions—I. Fatty acid adsorption. *Geochim. Cosmochim Acta.* **52,** 1667–1678.

Appendix Table I. Composition of equilibrium $CaCO_3(s)$ - $CaCO_3(aq)$ solutions

$CaCO_3$ (aq) Solutions with $PCO_2 = 10^{-3.5}$ atm								
pH	Ca	Na	DIC	ClO_4	K	Mg	Si	Sr
	(mol/L)							
7.25	7.11E-2	5.87E-6	2.67E-4	1.29E-1	6.4E-5	6.6 E-4	1.2 E-4	4.0E-6
7.48	2.19E-2	6.35E-2	3.71E-4	9.59E-2	3.3E-5	2.01E-4	9.6E-5	1.4E-6
7.71	7.14E-3	8.57E-2	6.05E-4	9.53E-2	3.1E-5	7.0E-5	3.6E-5	4.3E-7
7.98	1.75E-3	9.44E-2	1.15E-3	8.61E-2	3.8E-5	9.9E-6	2.0E-5	1.4E-7
8.40	3.14E-4	9.35E-2	2.68E-3	8.58E-2	2.2E-5	BD*	2.6E-6	6.0E-8
8.60	8.21E-5	9.66E-2	5.39E-3	8.21E-2	2.6E-5	BD	2.0E-6	BD
8.88	3.27E-5	9.92E-2	1.03E-2	7.95E-2	3.3E-5	5.8E-6	3.6E-6	6.0E-8
9.22	1.21E-5	1.06E-1	2.25E-2	7.36E-2	2.6E-5	BD	3.2E-6	6.0E-8

*BD = below detection

Appendix Table II. Aqueous speciation reactions with associated equilibrium constants

Reaction	log K_r 25°C, I=0	Source
$Ca^{2+} + H_2O = CaOH^+ + H^+$	-12.6	BALL *et al.* (1981)
$Ca^{2+} + CO_3^{2-} = CaCO_3^o$	3.15	BALL *et al.* (1981)
$Ca^{2+} + H^+ + CO_3^{2-} = CaHCO_3^+$	11.3	BALL *et al.* (1981)
$H^+ + CO_3^{2-} = HCO_3^-$	10.3	BALL *et al.* (1981)
$2H^+ + CO_3^{2-} = H_2CO_3$	16.65	BALL *et al.* (1981)
$Na^+ + H^+ + CO_3^{2-} = NaHCO_3^o$	10.08	BALL *et al.* (1981)
$Na^+ + CO_3^{2-} = NaCO_3^-$	1.26	BALL *et al.* (1981)
Zinc		
$Zn^{2+} + H_2O = ZnOH^+ + H^+$	-8.96	BAES and MESMER (1976)
$Zn^{2+} + 2H_2O = Zn(OH)_2^o + 2H^+$	-16.9	BAES and MESMER (1976)
$Zn^{2+} + 3H_2O = Zn(OH)_3^- + 3H^+$	-28.4	BAES and MESMER (1976)
$Zn^{2+} + 4H_2O = Zn(OH)_4^{2-} + 4H^+$	-41.4	BAES and MESMER (1976)
$Zn^{2+} + H^+ + CO_3^{2-} = ZnHCO_3^+$	11.7	RYAN and BAUMAN (1978)
$Zn^{2+} + CO_3^{2-} = ZnCO_3^o$	4.76	BILINSKI *et al.* (1976)
Strontium		
$Sr^{2+} + H_2O = SrOH^+ + H^+$	-13.18	WAGMAN *et al.* (1982)
Nickel		
$Ni^{2+} + H_2O = NiOH^+$	-9.86	BAES and MESMER (1976)
$Ni^{2+} + 2H_2O = Ni(OH)_2^o + 2H^+$	-19.0	BAES and MESMER (1976)
$Ni^{2+} + H^+ + CO_3^{2-} = NiHCO_3^+$	12.52	FOUILLAC and CRIAUD (1984)
$Ni^{2+} + CO_3^{2-} = NiCO_3^o$	4.83	FOUILLAC and CRAIUD (1984)
Barium		
$Ba^{2+} + H_2O = BaOH^+ + H^+$	-13.36	BAES and MESMER (1976)
Cobalt		
$Co^{2+} + H_2O = CoOH^+ + H^+$	-9.67	BAES and MESMER (1976)
$Co^{2+} + 2H_2O = Co(OH)_2^o + 2H^+$	-18.76	BAES and MESMER (1976)
$Co^{2+} + 3H_2O = Co(OH)_3^- + 3H^+$	-32.23	SMITH and MARTELL (1976)
$Co^{2+} + 3H_2O = Co(OH)_4^{2-} + 4H^+$	-45.78	SMITH and MARTELL (1976)
$Co^{2+} + H^+ + CO_3^{2-} = CoHCO_3^+$	12.5	FOUILLAC and CRIAUD (1984), ZHOROV *et al.* (1976)
$Co^{2+} + CO_3^{2-} = CoCO_3^o$	4.41	COSOVIC et al. (1982) FOUILLAC and CRIAUD (1984)
Cadmium		
$Cd^{2+} + H_2O = CdOH^+ + H^+$	-10.08	BAES and MESMER (1976)
$Cd^{2+} + H^+ + CO_3^{2-} = CdHCO_3^+$	12.30	FOUILLAC and CRIAUD (1984)
$Cd^{2+} + CO_3^{2-} = CdCO_3^o$	4.00	DAVIS *et al.* (1987)
Manganese		
$Mn^{2+} + H_2O = MnOH^+ + H^+$	-10.59	BAES and MESMER (1976)
$Mn^{2+} + H^+ + CO_3^{2-} = MnHCO_3^+$	11.57	LESHT and BAUMAN (1978)
$Mn^{2+} + CO_3^{2-} = MnCO_3^o$	4.10	FOUILLAC and CRIAUD (1984)

Appendix Table III. Solubility reactions and associated equilibrium constants

Reaction	Log K 25°C, I=0	Source
$Ba^{2+} + CO_3^{2-} = BaCO_3(s)$	8.58	WAGMAN *et al.* (1982)
$Ca^{2+} + CO_3^{2-} = CaCO_3(s)$	8.48	BALL *et al.* (1981)
$Cd^{2+} + CO_3^{2-} = CdCO_3(s)$	12.1	RAI *et al.* (1991)
$Co^{2+} + CO_3^{2-} = CoCO_3(s)$	10.1	NAUMOV *et al.* (1974)
$Co^{2+} + 2H_2O = Co(OH)_2(s) + 2H^+$	-12.1	NAUMOV *et al.* (1974)
$Mn^{2+} + CO_3^{2-} = MnCO_3(s)$	10.4	JOHNSON (1982)
$Ni^{2+} + CO_3^{2-} = NiCO_3(s)$	6.34	WAGMAN *et al.* (1982)
$Ni^{2+} + 2H_2O = Ni(OH)_2(s) + 2H^+$	-10.8	BAES and MESMER (1976)
$Sr^{2+} + CO_3^{2-} = SrCO_3(s)$	9.27	PLUMMER and BUSENBERG (1987)
$Zn^{2+} + CO_3^{2-} = ZnCO_3(s)$	10.8	SCHINDLER *et al.* (1969)
$5Zn^{2+} + 2CO_3^{2-} + 6H_2O =$ $Zn_5(OH)_6(CO_3)_2(s) + 6H^+$	-9.65	SCHINDLER *et al.* (1969)